05,04

Comparison of magnetic properties of $GdFe_3(BO_3)_4$, ferroborates grown using various solvents

© I.A. Gudim, E.V. Eremin, N.V. Mikhashenok, V.R. Titova

Kirensky Institute of Physics, Federal Research Center KSC SB, Russian Academy of Sciences, Krasnoyarsk, Russia

E-mail: eev@iph.krasn.ru

Received October 25, 2022
Revised October 25, 2022
Accepted November 1, 2022

$GdFe_3(BO_3)_4$, single crystals were grown from melt-solutions based on bismuth trimolybdate and lithium tungstate. Single crystals of gadolinium ferroborate from lithium-tungstate solution-melt were grown for the first time. The magnetic properties of the grown crystals are compared. It is shown that the $GdFe_3(BO_3)_4$, ferroborate obtained using bismuth solution-melt trimolybdate contains impurities of Bi^{3+} ions (6% at.), which replace Gd^{3+} ions. Whereas $GdFe_3(BO_3)_4$, ferroborate grown from a solution-melt based on lithium tungstate does not seem to contain such uncontrolled impurities.

Keywords: crystal growth, antiferromagnets, multferroics.

DOI: 10.21883/PSS.2023.02.55406.505

1. Introduction

In recent years, rare-earth ferroborates with a huntite structure with a general formula $ReFe_3(BO_3)_4$ ($Re = Y$, La–Lu) have been in focus of researchers due to the multiferroic properties found in them [1–7]. The main element of the rare-earth ferroborate crystal structure (space group R32 at high temperatures) is spiral chains of edge-sharing FeO_6 octahedra oriented along the c (third-order) axis.. In the crystal structure of these compounds, the exchange coupling inside a chain is much stronger than the interchain coupling.

Magnetically, ferroborates are antiferromagnets with two (rare-earth and iron) interacting magnetic subsystems. The iron subsystem is ordered at $T_N = 30-40$ K. The rare-earth subsystem is magnetized by the $f-d$ interaction and essentially contributes to the magnetic anisotropy and orientation of magnetic moments.

The first technique developed for growing isostructural nonlinear-optical trigonal $ReAl_3(BO_3)_4$, aluminoborate crystals was based on using melt-solutions based on $K_2Mo_3O_{10} - B_2O3$ potassium trimolybdate [8]. Then, it was proposed to grow the $ReAl_3(BO_3)_4$ and $ReFe_3(BO_3)_4$ single crystals using new melt-solutions based on $Bi_2Mo_3O_{12} - B_2O_3$ bismuth trimolybdate [9]. In these melt-solutions Bi_2O_3 and MoO_3 are coupled stronger than K_2O_3 and MoO_3. Therefore, the substitution of bismuth and molybdenum in the grown crystal for the rare-earth element was assumed to be relatively weak [10]. However, as it was shown in [11] by chemical analysis and structural studies for the $GdFe_3(BO_3)_4$ ferroborate, Bi^{3+} ions replace the rare-earth ion in an amount up to 5% at., which is nevertheless smaller as compared with substitution of potassium and molybdenum [10]. At that time, the lithium tungstate-based melt-solutions were proposed.

It is well-known that the oxide compounds containing Bi^{3+} ions (or Pb^{2+} ions) have an unbound electron pair on the s-shell and can establish the conditions for the occurrence of local dipoles in the crystal structure, which inevitably affects the electrical properties of the compound [12], and, perhaps, its magnetic properties as well.

For example, previously the magnetic studies in $SmFe_3(BO_3)_4$ has shown that the use of a bismuth trimolybdate-based solvent results in the situation when the impurity of Bi^{3+} ions in minor quantities (approximately 5% at.) replaces the Sm^{3+} ions. While the use of lithium tungstate-based solvent allows growing more pure $SmFe_3(BO_3)_4$ ferroborate [13].

The aim of this study was to investigate the effect of the Bi^{3+} ion impurity on the magnetic properties of rare-earth $GdFe_3(BO_3)_4$ ferroborates grown from two different melt-solutions: based on $Li_2WO_4-B_2O_3$ lithium tungstate and based on $Bi_2Mo_3O_{12}-B_2O_3$ bismuth trimolybdate.

2. Preparation of samples and measurement procedure

Crystals of $GdFe_3(BO_3)_4$ gadolinium ferroborate were among the first crystals used by the authors to develop the techniques to grow single-crystal huntites [8,14]. A well-known solvent based on the K_2MoO_4 potassium molybdate was used to grow them. These crystals have been studied quite widely [15,16]. However, as it was shown by optical studies, quite large amounts of impurities of both potassium and molybdenum are recorded in the crystals grown in this way [10].

The authors of this study have proposed another solvent to grow crystals of rare-earth ferroborates with a structure of huntite. It is based on $Bi_2Mo_3O_{12}$ bismuth trimolybdate. Single-crystals of trigonal gadolinium ferroborate were grown from the $Bi_2Mo_3O_{12}-B_2O_3-Gd_2O_3-Fe_2O_3$ system. The comparative study [10] has shown that crystals grown from such system contain bismuth and molybdenum ions impurities, although in a considerably lower quantities than those grown from the system with potassium molybdate. Moreover, it is possible to almost get rid of the bismuth impurity by introducing a small (7–10%) excess of molybdenum. But the amount of the molybdenum itself in the crystal does not increase in this case.

However, it would by desirable to get rid of the residual impurities as well, and for this purpose one more solvent based on lithium tungstate was proposed.

For each melt-solution system we have determined a sequence of crystallizing phases and its dependence on the ratio of solvent components. In the case when potassium molybdate or bismuth trimolybdate or lithium tungstate was used as a solvent, hematite (α-Fe_2O_3) proved to be the only crystallizing phase containing iron. When adding boron oxide to the solvent, this phase was replaced by $FeBO_3$ and Fe_3BO_6 iron borates. And only with the introduction of hyperstoichiometric gadolinium oxide to the solvent, it became possible to achieve the situation when the only high-temperature crystallizing phase is the trigonal gadolinium ferroborate in a quite wide temperature range, over 100°C.

The investigated melt-solution systems can be expressed in the quasi-binary form:

$$(100-n)\%\text{wt.}\,[K_2MoO_4 + pB_2O_3 + qGd_2O_3] + n\%\,\text{wt.}\,GdFe_3(BO_3)_4, \quad (a)$$

$$(100-n)\%\,\text{wt.}\,[Bi_2Mo_3O_{12} + pB_2O_3 + qGd_2O_3] + n\%\,\text{wt.}\,GdFe_3(BO_3)_4, \quad (b)$$

$$(100-n)\%\,\text{wt.}\,[Bi_2Mo_3O_{12} + pB_2O_3 + mMoO_3 + qGd_2O_3] + n\%\,\text{wt.}\,GdFe_3(BO_3)_4, \quad (c)$$

$$(100-n)\%\,\text{wt.}\,[Li_2WO_4 + pB_2O_3 + qGd_2O_3] + n\%\,\text{wt.}\,GdFe_3(BO_3)_4. \quad (d)$$

Table 1 shows ratios of solvent components and saturation temperature.

To avoid the impact of process factors on the properties of grown crystals, they were grown following a single procedure.

The 150 g melt-solution weights were prepared by melting together the mix of components at a temperature of 1050°C followed by exposure for 24 h for homogenization. During this time the melt-solution was mixed by a rod holder at a speed of 60 rpm.

Then the furnace temperature was decreased down to $T = 950$°C and after exposure for 20 h the crystal formation on the rod was evaluated. In all cases we obtained spontaneous crystals, which were then used to refine the saturation temperature (T_{sat}). Crystals of the most high quality were used as seeds. 4–6 such seeds were secured on the rod crystal holder.

Table 1. Composition of melt-solutions

Melt-solution	n	p	q	m	T_{sat}, °C
1	30	2	0.4		980
2	28	2.5	0.5		960
3	27	3	0.5	0.05	976
4	12	3	0.3		990

Table 2. Program of temperature decrease in the furnace

№ days	1	2	3	4	5	6	7	8	9	10
dT/Dt, °C/day	0	1	1	1	1	1.5	1.5	2	2	2

After the intermediate homogenization at $T = 1050$°C for 16–20 h, the furnace temperature was decreased down to $T = T_{sat} + 7$°C. The crystal holder with seeds was placed into the furnace and soaked for 0.25 h above the melt-solution. Then it was immersed to the melt-solution and after 0.25 h the furnace temperature was decreased by 14°C. Further temperature decrease was performed with increasing rate from 0 to 3°C/day (Table 2).

The duration of growth was from 7 to 10 days. During this time crystals grew up to a size from 5 to 7 mm with their quality allowing for comprehensive investigation of properties.

The magnetic study was carried out on a PPMS Quantum Design (research equipment sharing center of the Federal Research Center of KSC SB RAS) in the temperature range of 4.2–300 K and magnetic fields of up to 9 T.

3. Results and discussion

Since in [11,13] it was shown, that with the use of bismuth trimolybdate as a solvent the Bi^{3+} ions are present in the crystal as an impurity, so in the following text crystals grown from this melt-solution are denoted as $GdFe_3(BO_3)_4$:Bi, while crystals grown from the melt-solution based on lithium tungstate are denoted as $GdFe_3(BO_3)_4$, because it is assumed that with this sort of solvent there must not be uncontrolled impurities.

The determination of magnetic structure in the holmium ferroborate presents certain challenges due to the strong absorption of neutrons by Gd^{3+} ions, which makes it very difficult to use the method of elastic neutron scattering to determine the magnetic structure.

As for the magnetic structure of gadolinium ferroborate, the literature has discrepant data. In [17], it was shown on the basis of antiferromagnetic resonance investigation, that the magnetic phase transformation of the Fe^{3+} ions subsystem occurring at the Neel point T_N corresponds to

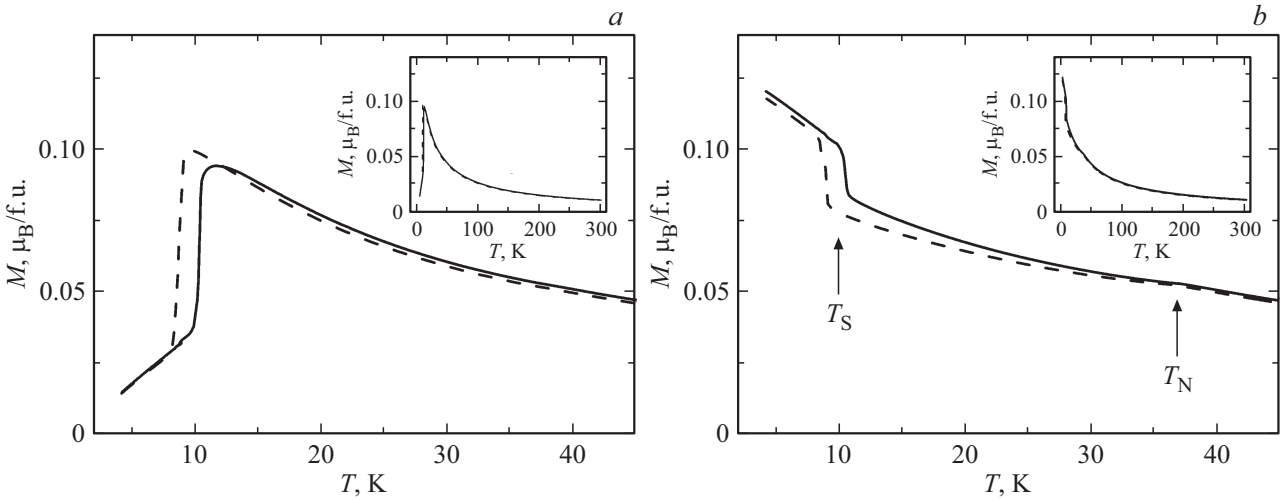

Figure 1. Temperature dependences of magnetization for $GdFe_3(BO_3)_4$ (solid curves) and $GdFe_3(BO_3)_4:Bi$ (dashed curves) measured in a magnetic field of 1 kOe and in a geometry of $B \parallel c$ (*a*) and $B \perp c$ (*b*). The inserts show the same in another scale.

the two-sublattice spin ordering of easy plane type. With a decrease in temperature below T_S, under the effect of interaction between iron and gadolinium subsystems a spin-flip transition from the easy-plane state to the easy-axis state takes place.

In [15] the magnetic behavior of gadolinium ferroborate was investigated in the framework of three-sublattice ordering (of the triangular type) of the iron subsystem. In this model spins of Fe^{3+} ions in the temperature range of $10\,K < T < 38\,K$ are lying in the „easy plane" at an angle of 120° to each other. Below 10 K, as a result of the interaction between iron and gadolinium subsystems, the Fe^{3+} spins are reoriented in the direction toward the easy axis, forming a cone with axis along *c*.

Further investigations using the x-ray resonant exchange scattering have shown that the magnetic ordering takes place at $T_N \approx 37\,K$ [18]. The magnetic structure becomes misfit below T_N with the misfitting degree monotonously decreasing with decrease in temperature until a transition to the fit magnetic phase occurs at $T \approx 10\,K$. Fe moments are spin-flipped at $T_{SR} \approx 9\,K$, so they become oriented along the crystallographic *c*-axis at low temperatures.

Our magnetic measurements confirm previous conclusions. Fig. 1 shows temperature dependencies of magnetization of the $GdFe_3(BO_3)_4$ single crystals grown with the use of various solvents: bismuth trimolybdate and lithium tungstate. The temperature dependencies of magnetization $M_\parallel$ and $M_\perp$ were measured in a magnetic field of 0.1 T directed along the crystallographic *c*-axis and in the basal plane along the *a*-axis, respectively.

In the paramagnetic region, the magnetization of both compositions is isotropic and obeys the Curie–Weiss law. The experimental paramagnetic Curie temperatures differ insignificantly and amount to respectively: $\theta = -45.7\,K$ for $GdFe_3(BO_3)_4$ and $\theta = -44.7\,K$ for $GdFe_3(BO_3)_4:Bi$. The negative sign is indicative of the antiferromagnetic exchange coupling in the magnetic system. It can be seen that the paramagnetic Curie temperature of $GdFe_3(BO_3)_4:Bi$ is lower, i.e. it decreases, as expected, upon substitution of magnetic Gd^{3+} ions by nonmagnetic Bi^{3+} bismuth ions. The effective magnetic moment of one structural unit of $GdFe_3(BO_3)_4$ appeared to be $\mu_{eff} = 12.96\mu_B$, which is exactly equal to the theoretic value of μ_{eff} determined as

$$\mu_{eff} = \sqrt{3 \cdot g_S^2 \cdot \langle S_{Fe}\rangle^2 \cdot \mu_B^2 + g_J^2 \langle J_{Gd}\rangle^2 \cdot \mu_B^2}, \qquad (1)$$

where $g_S = 2$ *g*-factor taking into account the spin moment only, $g_J = 2$ — Lande factor for Gd^{3+} ion, $\langle S_{Fe}\rangle^2 = S \cdot (S+1)$ — squared operator of the spin moment of the iron ion ($S = 5/2$ for Fe^{3+}), $\langle S_{Gd}\rangle^2 = J \cdot (J+1)$ — squared operator of the total moment of the gadolinium ion ($J = 7/2$ for Gd^{3+}).

On the other hand, the effective magnetic moment of one structural unit of $GdFe_3(BO_3)_4:Bi$ appeared to be $\mu_{eff} = 12.8\mu_B$, which is slightly lower than the theoretically determined value of μ_{eff}. By assuming that Gd^{3+} ions are replaced by Bi^{3+} ions and using the difference in values of μ_{eff} for $GdFe_3(BO_3)_4$ and $GdFe_3(BO_3)_4:Bi$, an estimate can be made of how much Bi^{3+} impurity was entered into the crystal matrix. In our case it appears that in $GdFe_3(BO_3)_4:Bi$ there are Bi^{3+} ions in an amount of 6% at.

With a decrease in temperature, at T_N (the Neel temperature) an ordering of the magnetic structure takes place. T_N can be determined quite precisely from Fig. 1, *b*. It is equal to $T_N = 37.1\,K$ for $GdFe_3(BO_3)_4$ and $T_N = 36.4\,K$ for $GdFe_3(BO_3)_4:Bi$, respectively. This again is indicative of the fact that the presence of Bi^{3+} ions results in a decrease in magnetic ordering. Then, with a decrease in temperature, a spin-flip transition is observed at $T_S = 10.5\,K$ for $GdFe_3(BO_3)_4$ and $T_S = 8.7\,K$ for $GdFe_3(BO_3)_4:Bi$. It is important to note that this transition is observed in both orientations of the magnetic field: $H \parallel c$ and $H \perp c$. This is indicative of the fact that this magnetic structure can not

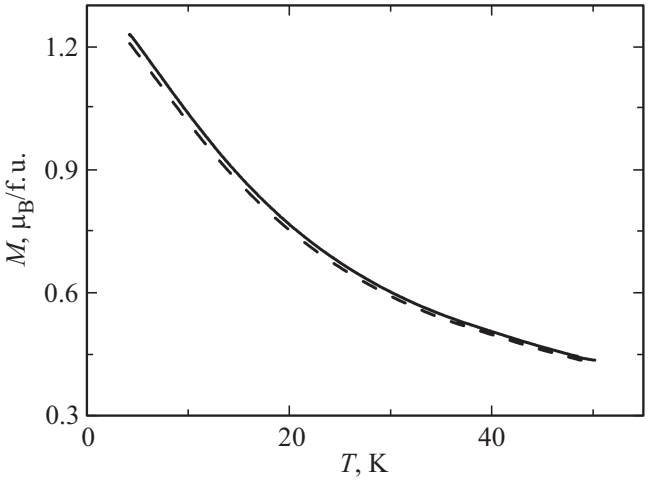

Figure 2. Temperature dependences of magnetization for $GdFe_3(BO_3)_4$ (solid curve) and $GdFe_3(BO_3)_4:Bi$ (dashed curve) measured in a magnetic field of 10 kOe and in a geometry of $B \parallel c$.

be considered as a classic two-sublattice antiferromagnetic. And the difference in transition temperatures of almost two degrees indicates once again that Bi^{3+} ions replace Gd^{3+} ions, since, for example, in the $YFe_3(BO_3)_4$ ferroborate (where magnetic subsystem is represented by Fe^{3+} ions only) there are no any spin-flip transitions. It's worth noting that the spin-flip transition takes place only in relatively weak fields. Thus, in a field of 10 kOe actually it is not observed any more (Fig. 2).

Field dependencies of magnetization M(H) for both compounds in the direction of magnetic field $H \parallel c$ and $H \perp c$ are shown in Fig. 3. It can be seen in Fig. 3, *a*, that as the magnetic field ($H \parallel c$) increases, a spin-flop transition takes place at $H_{SP1} = 7.4$ kOe for $GdFe_3(BO_3)_4$ and $H_{SP1} = 6.4$ K for $GdFe_3(BO_3)_4:Bi$, respectively. In the case of $H \perp c$ magnetic field orientation, also a spin-flip transition induced by magnetic field is observed, but at higher fields: $H_{SR2} \approx 40$ kOe for $GdFe_3(BO_3)_4$ and $H_{SR2} \approx 35$ K for $GdFe_3(BO_3)_4:Bi$, respectively. Here, again, a trend of transition temperature decrease can be seen as Gd^{3+} ions are replaced by Bi^{3+} ions.

Thus, the magnetic investigation shows that in crystals of $GdFe_3(BO_3)_4$ ferroborate grown with the use of bismuth trimolybdate-based melt-solution Bi^{3+} ions replace Gd^{3+} ions in an amount of 6% at. and have a significant effect on magnetic properties of the grown crystals.

4. Conclusion

$GdFe_3(BO_3)_4$ single crystals were grown from the lithium tungstate-based melt-solution for the first time. For the purpose of comparison, $GdFe_3(BO_3)_4$ single crystals were grown with the use of a solvent based on bismuth trimolybdate. A comparative analysis of magnetic properties of these ferroborates is carried out.

It follows from the magnetic investigation that the use of bismuth trimolybdate-based solvent results in the situation when Bi^{3+} ions in small amounts (6% at.) replace Gd^{3+} ions. While the use of the solvent based on lithium tungstate gives the possibility to grow more pure $GdFe_3(BO_3)_4$ ferroborate, that can be seen, for example, when determining the effective magnetic moment from the Curie–Weiss law, which is precisely match the theoretically calculated value.

Funding

This study was supported by grant No. 22-12-20019 provided by the Russian Science Foundation and the Krasnoyarsk Regional Science Foundation (https://rscf.ru/project/22-72-00017/).

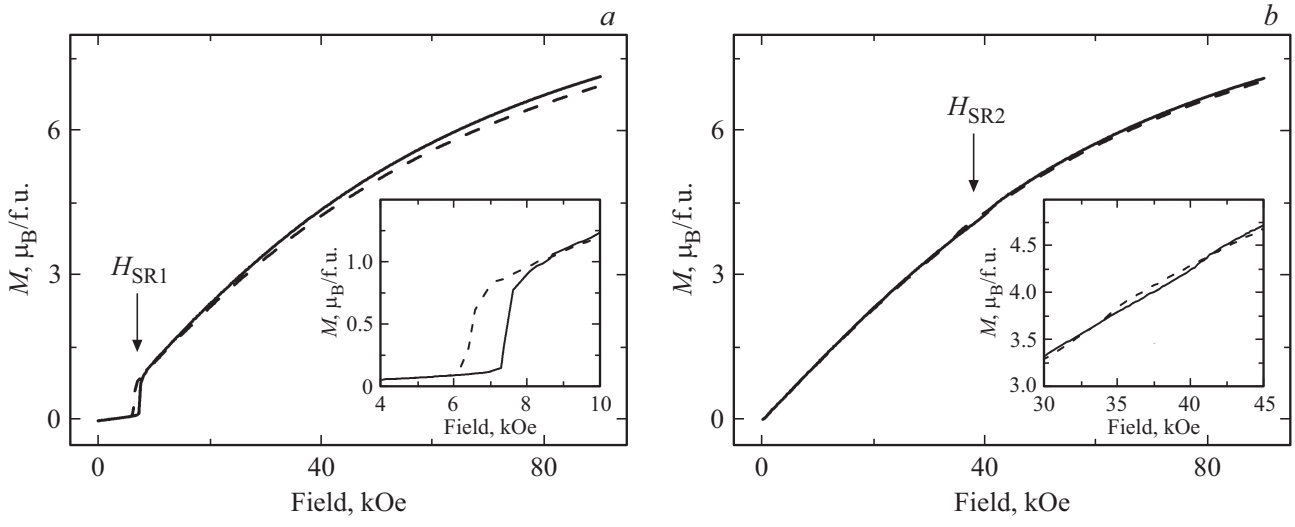

Figure 3. Field dependences of magnetization for $GdFe_3(BO_3)_4$ (solid curves) and $GdFe_3(BO_3)_4:Bi$ (dashed curves) measured at a temperature of 4.2 K and in a geometry of $B \parallel c$ (*a*) and $B \perp c$ (*b*). The inserts show the same in another scale.

Conflict of interest

The authors declare that they have no conflict of interest.

References

[1] A.K. Zvezdin, S.S. Krotov, A.M. Kadomtseva, G.P. Vorob'ev, Yu.F. Popov, A.P. Pyatakov, L.N. Bezmaternykh, E.A. Popova, Pis'ma v ZhETF **81**, *6*, 335 (2005) (in Russian).
[2] A.M. Kadomtseva, Yu.F. Popov, G.P. Vorob'ev, A.P. Pyatakov, S.S. Krotov, K.I. Kamilov, V.Yu. Ivanov, A.A. Mukhin, A.K. Zvezdin, A.M. Kuz'menko, L.N. Bezmaternykh, I.A. Gudim, V.L. Temerov, FNT **36**, *6*, 640 (2010) (in Russian).
[3] R.P. Chaudhury, F. Yen, B. Lorenz, Y.Y. Sun, L.N. Bezmaternykh, V.L. Temerov, C.W. Chu. Phys. Rev. B **80**, *10*, 104424 (2009).
[4] A.N. Vasiliev, E.A. Popova, FNT **32**, *8/9*, 968 (2006) (in Russian).
[5] V.I. Zinenko, M.S. Pavlovskiy, A.S. Krylov, I.A. Gudim, E.V. Eremin, ZhETF **144**, *6*, 1174 (2013) (in Russian).
[6] A.P. Pyatakov, A.K. Zvezdin, UFN **182**, *6*, 593 (2012) (in Russian).
[7] T. Usui, Y. Tanaka, H. Nakajima, M. Taguchi, A. Chainani, M. Oura, S. Shin, N. Katayama, H. Sawa, Y. Wakabayashi, T. Kimura. Nature Mater. **13**, *6*, 618 (2014)
[8] N.I. Leonyuk L.I. Leonyuk. Prog. Cryst. Growth Charact. **31**, 179 (1995).
[9] L.N. Bezmaternykh, V.L. Temerov, I.A. Gudim, N.A. Stolbovaya. Crystallogr. Rep. **50**, *S1*, 97 (2005).
[10] K.N. Boldyrev, M.N. Popova,M. Bettinelli, V.L. Temerov, I.A. Gudim, L.N. Bezmaternykh, P. Loiseau, G. Aka, N.I. Leonyuk. Opt. Mater. **34**, *11*, 1885 (2012).
[11] I.S. Lyubutin, A.G. Gavriliuk, N.D. Andryushin, M.S. Pavlovskiy, V.I. Zinenko, M.V. Lyubutina, I.A. Troyan, E.S. Smirnova. Cryst. Growth Des. **19**, *12*, 6935 (2019).
[12] R. Seshadri, G. Baldinozzi, C. Felser, W. Tremel. J. Matter. Chem. **9**, 2463 (1999).
[13] E. Eremin, I. Gudim, V. Temerov, D. Smolyakov, M. Molokeev. J. Cryst. Growth **518**, 1 (2019).
[14] N.I. Leonyuk. Prog. Cryst. Growth Charact. **31**, 279 (1995).
[15] A.D. Balaev, L.N. Bezmaternykh, I.A. Gudim, V.L. Temerov, S.G. Ovchinnikov, S.A. Kharlamova. J. Magn. Magn. Mater. **258**–**259**, 532 (2003).
[16] A.M. Kadomtseva, Yu.F. Popov, S.S. Krotov, A.K. Zvezdin, G.P. Vorob'ev, L.N. Bezmaternykh, E.A. Popova, FNT **31**, *8/9*, 1059 (2005) (in Russian).
[17] A.I. Pankrats, G.A. Petrakovsky, L.N. Bezmaternykh, O.A. Bayukov, ZhETF **246**, *10*, 887 (2004) (in Russian).
[18] H. Mo, C.S. Nelson, L.N. Bezmaternykh, V.L. Temerov. Phys. Rev. B **78**, 214407 (2008).

Translated by Ego Translating